Int J Adv Manuf Technol (2018) 94:2267–2280
DOI 10.1007/s00170-017-0987-5

ORIGINAL ARTICLE

Shape optimization methodology of clinching tools based on Bezier curve

Meng-han Wang[1] · **Gui-qian Xiao**[1] · **Zhi Li**[1] · **Jin-qiang Wang**[1]

Received: 12 April 2017 / Accepted: 14 August 2017 / Published online: 6 September 2017

Abstract The purpose of this paper is to propose a methodology for the strength optimization of mechanical clinched joint. To this end, a mathematical optimization model which introduces ductile damage constraint to prevent the onset of fracture during the clinch joining of thin metal sheets is proposed. Meanwhile, Bezier curve is used to describe the outline shape of the clinching die, which can be used to search a lot of potential shapes by changing the location of the control point. In addition, a new solving method based on the direct communication between FE-analysis and genetic algorithm (GA) is proposed. The results indicate that the shape of the die groove can be replaced by arc curve to simplify the structure of the clinching tools for general applications. If the requirement of the joint strength is not very high or the ductility of the sheet is good, the clearance between the lower sheet and the die groove is not necessarily equal to zero, but if the requirement is very high or the ductility is poor, the zero clearance is very necessary.

Keywords Mechanical clinching · Shape optimization · Genetic algorithm · Bezier curve

✉ Meng-han Wang
cquwmh@163.com

✉ Gui-qian Xiao
xgq3790@163.com

[1] School of Material Science and Engineering, Chongqing University, Chongqing 400044, China

1 Introduction

Many lightweight materials are widely used to reduce the weight of structure. Typically, aluminum and magnesium alloy are more and more popular due to low density, anticorrosion, and excellent mechanical performance. Conventional wielding techniques are not suitable for these kinds of materials [1]. Therefore, some mechanical joining techniques have been developed for joining the advanced lightweight materials that are dissimilar, coated, and hard to weld [2]. Particularly, mechanical clinching has numerous advantages, such as low run time, low cost per joint, absence of subsidiary, simplicity, and cleanness [3]. The first patent related to the clinching was granted as early as 1897 [4, 5], which has been widely used to join many materials, such as high-strength metals [6–8], polymers [9–11], and composite [12–14]. The main limitation of clinching is the lower joint strength. For those materials with poor formability, such as high-strength steel, the improvement of the formability is the main method to improve the joint strength. The formability of materials can be increased by means of heating systems [15–17] or die design [18]. For those materials with good formability, such as aluminum alloy, the die design is the main method to improve the joint strength. Varis [19] pointed out that round joint appears to have good mechanical performance. Results from Lambiase [3, 20] indicate that punch diameter, punch corner radius, fixed die depth, fixed die diameter, and die corner have a significant influence on joint strength. Oudjene and Ben-Ayed [21] pointed out that the resistance of the clinch joint highly depends on the joint shape and can be greatly improved by optimizing the influential parameters.

In order to further improve joint strength, some methods have been developed. Lambiase and Di Ilio [22] developed an optimization model of the clinching tools based on artificial intelligence techniques and FE-analysis, in which the artificial

neural network (ANN) was used to approximate the response relationship between joint strength and tools geometry, and genetic algorithm (GA) was utilized to optimize this response model. The joint strength was increased significantly by this way. Roux and Bouchard [23] optimized the geometry parameters of the clinching tools by using Kriging meta-model. The strength of the clinching component has been increased by 13.5%. Oudjene et al. [24] optimized the clinching tools by means of response surface methodology (RSM) combined with moving least-square approximation. It is an efficient way to improve the joint strength. Lebaal et al. [25] proposed a modified Kriging meta-model. Their results indicate that the use of the Kriging meta-model is an effective way to improve the convergence performance. These design methods show a good ability to obtain the best clinched joint, and it is also an effective way for engineering application.

However, there is an undeniable fact that the global optimum solution still can be lost easily. On the one hand, the approximate response model, especially for multivariable problem, cannot be accurately established by using few times of simulation. On the other hand, the design variables are just specified as the geometry parameters of the clinching tools, by which some potential shapes cannot be searched. The aim of this paper is to establish a systematic methodology for optimizing the strength of the clinched joint. Firstly, a mathematical model for the optimization of the clinched joint is developed, and corresponding solving algorithm based on the direct communication between FE-analysis and GA is established. Secondly, Bezier curve is applied to describe the shape of the clinching die, by which many potential shapes can be searched. The location of the control points and other geometry parameters are defined as the design variables. GA module is used as a controller to control these design variables. Therefore, the best shape of clinching tools can be preserved through crossover, variation, and competing among all individuals. Finally, Al6061-T4 sheets are used to verify the feasibility of the optimization methodology. In addition, four different initial shapes are used to investigate the evolutionary process and to explore the global optimum shape of the die groove.

2 Analytic formulas for joint strength

The failures of clinched joint are axial failure and shear failure. Axial failure can be divided into two modes: button separation and neck fracture (see Fig. 1a, b). Shear strength of clinched joint only depends on shear failure (see Fig. 1c). Therefore, the strength of clinched joint is mainly determined by the three failure modes which are discussed carefully in the next section.

2.1 Axial strength

The typical failure mode in axial direction is neck fracture and button separation (Fig. 1a, b). According to some research [5, 26–28], axial strength can be predicted by analytical formulas. The computation time can be reduced dramatically, and the accuracy can also be improved significantly by this way. The analytical formulas are adopted to calculate the joint strength in this paper. It is known that clinched joint can be characterized by the following parameters: neck thickness (t_n), interlocking length (t_u), inner diameter (d), and inclination angle (θ) (see Fig. 2). Then, joint strength can be defined as a function of t_n, t_u, d, and θ.

2.1.1 Button separation failure

Button separation failure is the separation of the upper sheet and the lower sheet due to insufficient geometrical interlocking (see Fig. 1a). Under axial loading, the upper sheet is separated vertically from the locking location to the outside of the joint. Chan-Joo Lee et al. [5] developed an analytical formula which was verified by their tensile experiments. The analytical formula for calculating the separation strength is used in this paper as follows:

$$F_{se}=\frac{\pi}{4}[\sigma]\left[(d+2t_n)^2-d^2\right]\left(\frac{\tan\theta+u}{u}\right)\left\{1-\left[\frac{(d+t_n)t_n}{(d+t_n+t_u)(t_n+t_u)}\right]^{\frac{u}{\tan\theta}}\right\} \tag{1}$$

where F_{se} is the failure strength of the button separation mode. $[\sigma]$ is the allowable stress which is equal to σ_s/n. σ_s is the yield strength of the upper sheet, and n is the safety factor. For different materials, the value of the safety factor is different. u is the friction coefficient between the two sheets, and F_{se} represents the axial tensile strength of the button separation failure.

2.1.2 Neck fracture failure

Neck fracture failure is the neck fracture phenomenon which is caused by the excessive plastic deformation in the neck region of the clinched joint (see Fig. 1b). Obviously, the strength of this mode is equal to the product of the area in the neck region and the tensile strength of the upper sheet. Therefore, the analytic formula can be listed as follows:

$$F_{fr}=[\sigma]S=\frac{\pi}{4}[\sigma]\left[(d+2t_n)^2-d^2\right] \tag{2}$$

where F_{fr} represents axial tensile strength of the button separation failure. $[\sigma]$ is the allowable stress which is equal to σ_s/n. σ_s is the yield strength of the upper sheet, and n is the safety

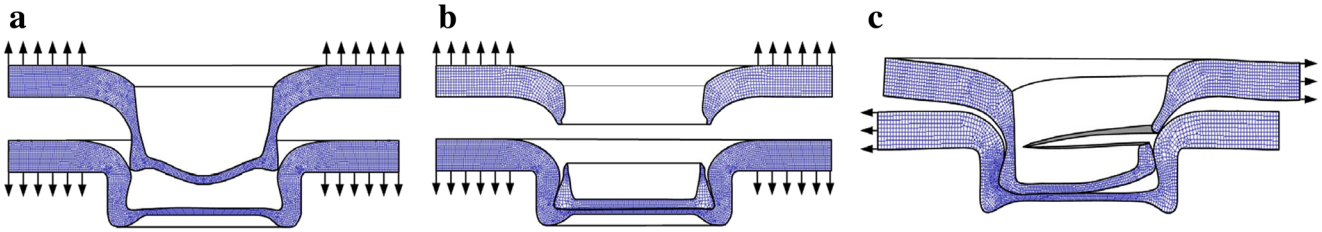

Fig. 1 Three basic failure modes: button separation (**a**), neck fracture mode (**b**), shear failure mode (**c**)

factor. For different materials, the value of the safety factor is different.

2.1.3 Shear failure

Shear failure is the neck fracture phenomenon which is caused by the shear stress (see Fig. 1c). This failure is dependent on the area of the neck region and the shear strength of the upper sheet. This strength can be defined as follows:

$$F_t = [\tau]S = \frac{[\sigma]}{\sqrt{3}}\frac{\pi}{4}\left[(d+2t_n)^2 - d^2\right] \tag{3}$$

where $[\sigma_s]$ is the allowable stress of the upper sheet which is equal to σ_s/n. σ_s is the yield strength of the upper sheet, and n is the safety factor. For different materials, the value of the safety factor is different. $[\tau]$ is the allowable shear stress of the upper sheet, and F_t is the shear strength of the joint.

2.2 Optimization methodology

The optimization of the clinched joint is to deal with the balance between three failure strengths. In other words, these three failure strengths cannot be increased synchronously. Hence, the relationship between these failure strengths will be discussed carefully in this section.

2.2.1 Objective function

Axial strength of the clinched joint depends not only on button separation mode but also on neck fracture mode, for there is only one failure mode triggered in a failure. To understand the relationship between two kinds of failure mode easily, the strength distribution for the two failure modes is displayed in Fig. 3.

As is shown in Fig. 3, the intersection of two surfaces is the optimum curve. With the increase of t_n and t_u, the value of the optimum curve is also increased. Unfortunately, it is extremely difficult or even impossible to make t_n and t_u to reach a large value synchronously. The axial strength of clinched joint is composed of two lower surfaces which are surrounded by solid lines. Therefore, axial strength of clinched joint can be defined as follows:

$$F_a = \min(F_{fr}, F_{se}) \tag{4}$$

where F_a denotes axial strength of clinched joint. The goal of this study is to maximize the axial strength. Therefore, the objective function can be defined as follows:

$$obj_a = \max(\min(F_{fr}, F_{se})) \tag{5}$$

where obj_a is the objective function of axial strength. As deduced in the previous section, F_{fr} and F_{se} are defined as a function of neck thickness (t_n), undercut (t_u), dip angle (θ), etc. Since the controllable parameters are not the joint's shape, these parameters cannot be defined as design variables. In fact, t_n, t_u, and θ are an unknown function of the tools' shape. Fortunately, this function relationship can be acquired by FE-analysis. In addition to axial strength, the shear strength is also important. Hence, the shear strength should be maximized as follows:

$$obj_t = \max(F_t) \tag{6}$$

where obj_t is the objective function of shear strength.

As shown in Fig. 4, the shear load can be equally divided by two joints, but the axial load cannot. Hence, the total shear strength of the structure can be improved by using more clinch joint, but the total axial strength cannot be improved.

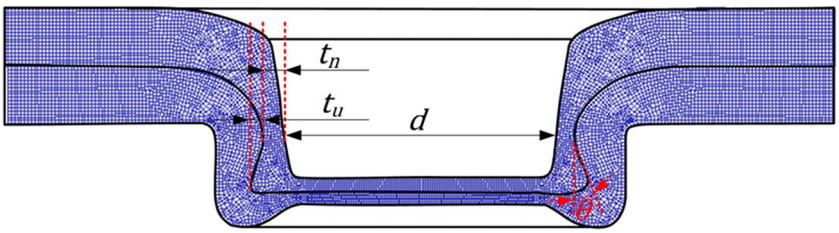

Fig. 2 Four feature parameters of clinched joint

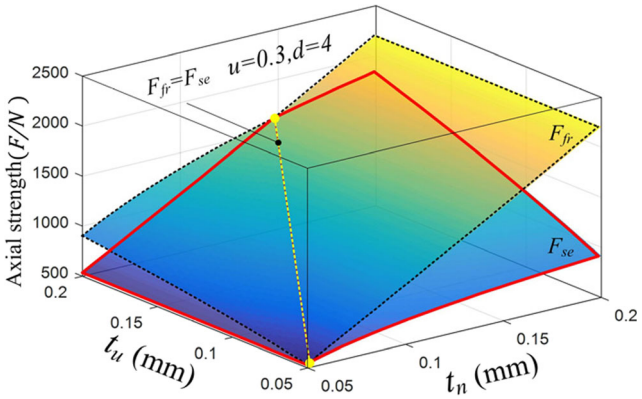

Fig. 3 Strength relationship between two kinds of axial failure mode

The reason is that thin sheet lacks ability to transfer bending moments under axial loading. Therefore, the importance of the axial strength is more than the shear strength, and the axial strength is mainly maximized in this paper.

2.2.2 Constraint conditions

In order to improve efficiency of the optimization algorithm, the feasible region of design variables should be defined as follows:

$$\boldsymbol{LB}^T \le [x_1, x_2 \cdots x_n]^T \le \boldsymbol{UB}^T \tag{7}$$

where $x_1, x_2 \cdots x_n$ are shape parameters of clinching tools which are shown in Fig. 7.

In order to obtain high-integrity joint, the damage of the material must be considered. According to some studies [1, 23], neck fractures in clinching process are caused by ductile damage. In this paper, the normalized Cockcroft and Latham's equation has been adopted. Therefore, the damage constraint can be defined as follows:

$$D = \int_0^{\bar{\varepsilon}_f} \frac{\sigma^*}{\overline{\sigma}} \bar{\varepsilon} \le C \tag{8}$$

where C is the damage threshold, and D is the maximum damage value of materials. Hambli and Reszka [29] used inverse technique method to identify suitable fracture criteria in blanking experiments. In this paper, the determination of the damage threshold is not the central task. Hence, the value of the damage threshold can be referred to relevant papers [28]. In addition, a computer program (MATLAB code) has been developed to extract the maximum damage value from Deform-2D's key file.

2.2.3 Mathematical optimization model

This model is a typical multi-objective optimization problem which can be translated to a single objective problem by weighting method or optimum seeking method. Since the importance of axial strength is far greater than shear strength. Hence, optimum seeking method will be adopted, by which $\max(F_t)$ is translated into a constraint condition. The optimization model for joint strength can be established as follows:

$$\begin{cases} Minimize - \min(F_{fr}, F_{se}) \\ s.t. \\ [t_n, t_u, \theta, d, D] = FEM\ (x_1, x_2 \cdots x_n) \\ F_t = \dfrac{F_{fr}}{\sqrt{3}} > k \\ D \le C \\ F_{fr} = \dfrac{\pi}{4}[\sigma]\left[(d+2t_n)^2 - d^2\right] \\ F_t = [\tau]\ S = \dfrac{[\sigma]}{\sqrt{3}}\dfrac{\pi}{4}\left[(d+2t_n)^2 - d^2\right] \\ F_{se} = \dfrac{\pi}{4}[\sigma]\left[(d+2t_n)^2 - d^2\right]\left(\dfrac{\tan\theta + u}{u}\right)\left\{1 - \left[\dfrac{(d+t_n)t_n}{(d+t_n+t_u)(t_n+t_u)}\right]^{\frac{u}{\tan\theta}}\right\} \\ with\ \boldsymbol{LB}^T \le [x_1, x_2 \cdots x_n]^T \le \boldsymbol{UB}^T \end{cases} \tag{9}$$

where k is the minimum value of the shear strength which can be specified by the user. FEM represents the finite element method. All of the other parameters are defined in the previous section. The most important fact is that $[\sigma]$ is shared by F_{fr}, F_t, and F_{se}. Therefore, the optimization results will not be affected by $[\sigma]$. Therefore, the working hardening can be ignored in this paper.

3 Solution strategy for optimization model

The search space created by the design variables ($x_1, x_2 \cdots x_n$) is very wide, and the gradient information of the design variables cannot be provided by FE-analysis. Therefore, regular optimization algorithms, such as

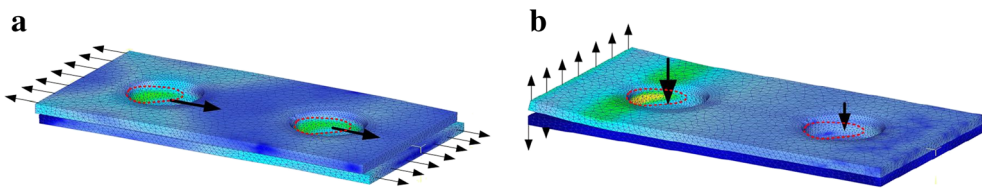

Fig. 4 Stress distribution in two loading directions: shear loading (**a**) and axial loading (**b**)

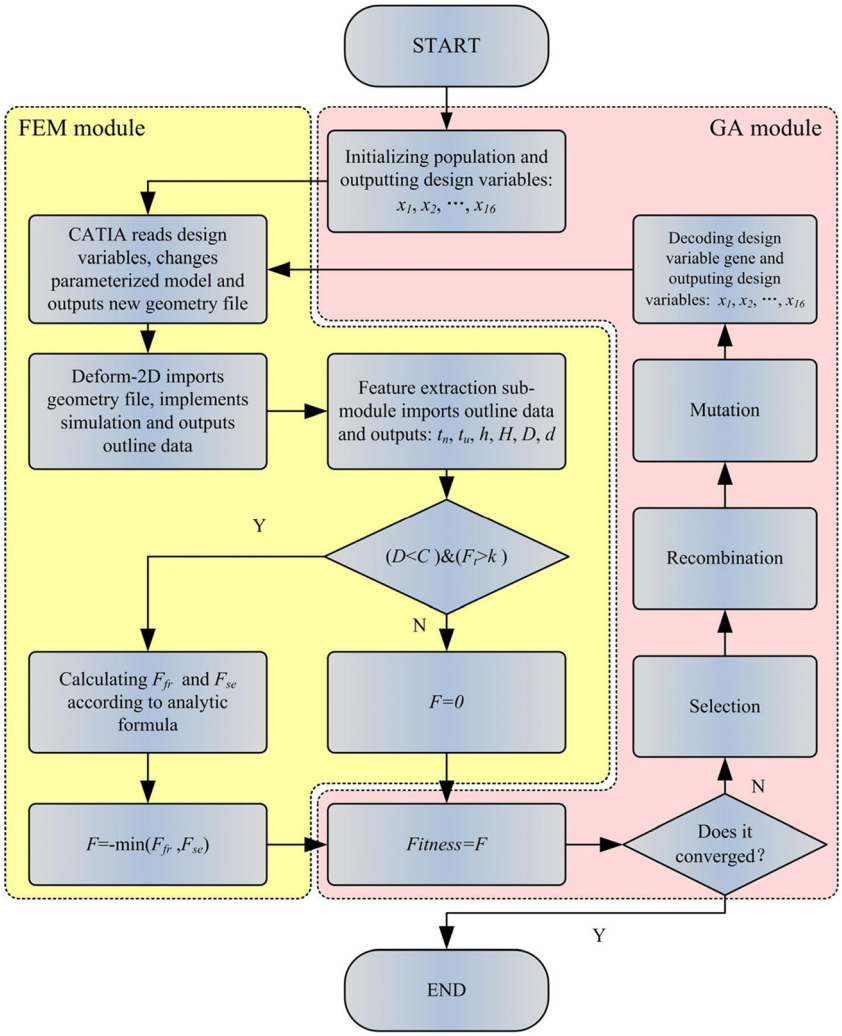

Fig. 5 Configuration of all modules

gradient methods or traversal research, are no longer suitable. For these reasons, GA is adopted because it does not need the gradient information, and it is well-adapted for a large number of optimization problems with large search spaces. GA simulates the phenomenon of natural evolution, in which design variables are encoded as individual. Each individual is so-called a chromosome represented by a binary bit string. The number of bits in the string is used to control the resolution of the design variables.

3.1 Algorithm structure

In the previous studies [9, 12], ANN and RSM are often used to approximate FE-analysis. In this paper, the direct communication between FEM and GA has been adopted. The GA module is used as a controller to send design variables to the FEM module and to receive individual fitness returned from the FEM module. Meanwhile, the FEM module serves as a calculator to simulate the clinching process using the design variables and to return the inverse number of the axial strength to the GA module as the fitness (see Fig. 5).

As shown in Fig. 5, the core modules in the algorithm flow chart are FEM module and GA module. There are several sub-modules included in the FEM module, such as numerical simulation sub-module, feature extraction sub-module, and strength calculation sub-modules.

3.1.1 Feature extraction sub-module

The function of feature extraction sub-module is extracting feature parameters (t_n , t_u , θ , d) by using joint shape data. The joint shape data can be obtained by using Deform-2D's point tracking function. As shown in Fig. 6a, there is no functional mapping relationship between x-coordinate and y-coordinate. For example, for a given x-coordinate on the curve, there are many y-coordinate mapped to this x-coordinate and vice versa. To overcome this problem, v, which is defined as the arc length from the origin of the coordinate system to a

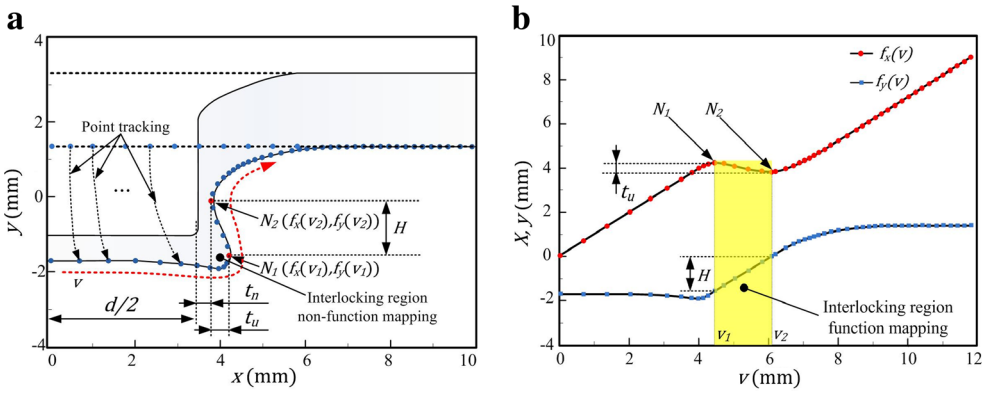

Fig. 6 Outline curve of joint (**a**) and its cumulative chord length parameterization curves (**b**)

given point, is introduced to build the parametric equations as follows:

$$v = \int_{(0,0)}^{(x,y)} \sqrt{dx^2 + dy^2} \tag{10}$$

As shown in Fig. 6b, there is a functional mapping relationship between x and v as well as y and v.The parameterization equation can be given as follows:

$$\begin{cases} x = f_x(v) \\ y = f_y(v) \end{cases} \tag{11}$$

where v is the introduced parameter and f_x, f_y are function which can be determined by using B-spline fitting method. It is very convenient to obtain N_1 and N_2 by using parametric equations. According to Calculus theory, the extreme value points of N_1 and N_2 can be determined by $\frac{dx}{dv} = 0$. Substituting v_1 and v_2 into $f_y(v)$, $f_y(v_1)$ and $f_y(v_2)$ can be obtained. Therefore, the calculation formula of the feature extraction algorithm can be developed as follows:

$$\begin{cases} \dfrac{dx}{dv} = 0 \Rightarrow v_1, \quad v_2 \\ t_u = |f_x(v_1) - f_x(v_2)| \\ tan\theta = \dfrac{t_u}{H} = \dfrac{|f_x(v_1) - f_x(v_2)|}{|f_y(v_1) - f_y(v_2)|} \\ t_n = \left| f_x(v_2) - \dfrac{d}{2} \right| \end{cases} \tag{12}$$

According to these formulas, corresponding computer code is programed to automatically extract the joint feature parameters.

3.1.2 Simulation sub-module

Although many studies have optimized the geometry parameters of the clinching tools, they have not optimized the shape of the clinching tools. A typical shape optimization is topology optimization in which the inner elements of a component can be removed or added. However, it is not necessary for the shape optimization of the clinching tools, because only surface of the clinching tools affects joint strength. Therefore, shape optimization of the clinching tools is just to deal with the outline shape of the tools. To solve this problem, the Bezier curve is used to describe the shape of the clinching die. It is generally known that the shape of the Bezier curve can be changed to approximate any shape by moving its control points.

The outline of die is described by the Bezier curve in the die groove (see Fig. 7 yellow region). The x-coordinate of control point is fixed, and its y-coordinate is defined as design variable. Comparing with traditional arc curve, the shape space can be searched more entirely by this way.

The shape of the die groove can be changed within a large range, which cannot only cover traditional shape (see Fig. 7) but also unconventional shape (see Fig. 8a–d). Therefore, the shape optimization problem can be

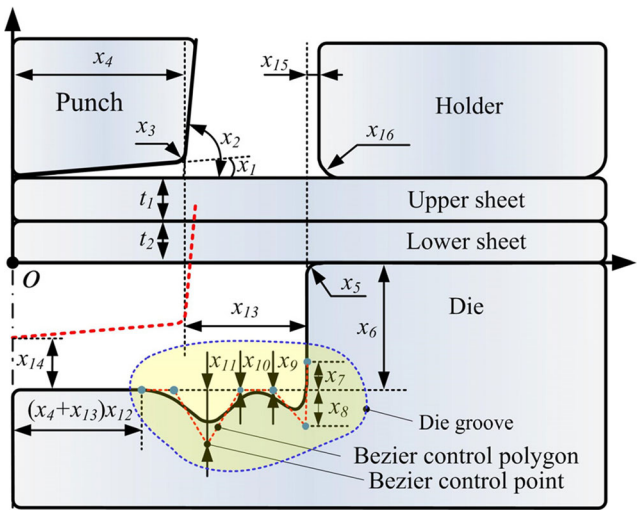

Fig. 7 Schematic representation of clinching tools with parameters

translated into the parameterization optimization problem by this way.

Deform-2D is used to simulate the clinching process, in which the skyline solver and the Newton-Raphson iteration method are adopted. The automatic re-meshing technology is also used to reduce the mesh distortion. In addition, a rigid plastic material model is used in the simulation. A fixed constraint is applied to the holder.

3.2 Parameter definition

The Al6061-T4 sheets with a thickness of 1.4 mm are used in the optimization process. The material properties are listed in Table 1. According to a study [28], the critical damage threshold value of Al6061-T4 is 1.61. The friction coefficient was assumed to be between 0.1 and 0.4 [5, 30]. In this study, the friction coefficients between tools and sheet were assumed to be 0.1 and the friction coefficient between upper and lower sheets was assumed to be 0.3.

In this paper, an individual is composed of 16 genes which represent the design variables. Rouffaud et al. recommended that the population size should hold 10 times of the gene number of individuals [31]. Hence, the population size should be assigned as 160. According to preliminary exploration, the population size is assigned as 100 to reduce the total time of the simulation in this paper. The crossover rate is set to 0.9, and the mutation rate is set to 0.1. The constraint condition is defined to increase the convergent rate and to ensure that crack does not occur in the clinching process.

$$\begin{cases} D < 1.61 \\ k = \dfrac{F_a}{2} \\ \boldsymbol{LB}^T = [0, 85, 0.2, 2.7, 0.2, 1.2, -0.2, 0, 0, 0, 0, 0.5, 1.4, 0.6, 1.0, 0.2] \\ \boldsymbol{UB}^T = [3, 90, 0.4, 4, 0.5, 2.5, 0.4, 0.6, 0.6, 0.6, 0.6, 0.8, 1.9, 1.2, 2.0, 0.5] \end{cases} \tag{13}$$

where k can be defined as a smaller value because the shear strength can be enhanced by using more clinched joint. In this paper, k is defined as $\frac{F_a}{2}$, by which the total shear strength of the structure is not less than its total axial strength if two joints are used. Of course, k can also be specified as other values if necessary. Although the initial population can be defined to reduce the optimization time according to user's experience, it is not defined to test the intelligence and robustness of the algorithm in the optimization process.

4 Results and discussion

4.1 Optimization results

According to the above analysis, an automatic optimization system has been developed. Using this system, the optimum results can be obtained after 700 (100 × 7) times of simulation, and the duration of the optimization is about 23 h (700 × 2 minutes min). As shown in Fig. 9b, the joint strength is gradually increased with the increase of generation. The objective function is not necessarily improved at 5th and 6th generation. This is due to the optimization algorithm which is global. Therefore, some computations are dedicated to the exploration of the design space. The fitness curve, the convergence curves, indicates that the objective is maximized by 43.68% compared to its initial value which is initialized by optimization system.

The evolutionary relationship between three failure strengths is illustrated in Fig. 9a. In the evolutionary process, F_{se} is always less than F_{fr}, and the F_{fr} is very close to the F_{se} at the 7th generation. As shown in Fig. 9a, the optimum solution is located in the region of $F_{fr} = F_{se}$, which is strongly agreed with the inference. After 700 times of simulation, the axial joint strength has been increased from 767 to 1100 N (see Fig. 9b), and the shear strength has been increased from 500 to 653 N (see Fig. 9a). The optimized design variables are given by Eq. (14).

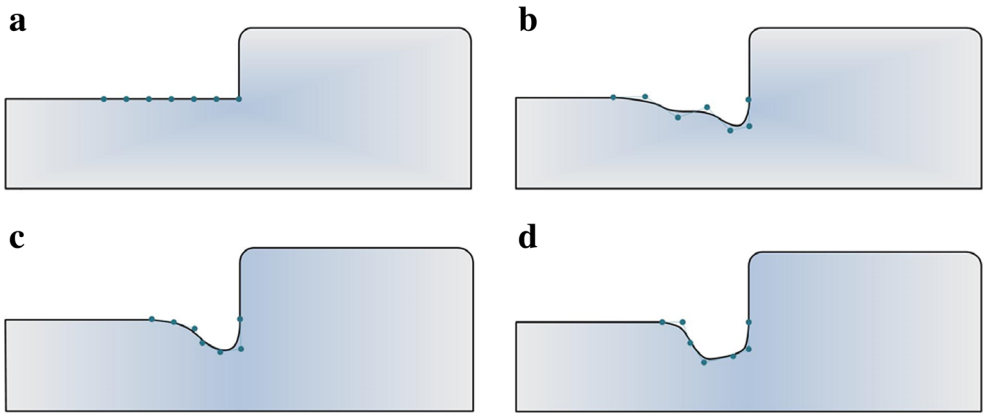

Fig. 8 Four typical shapes of die

Table 1 Material properties of Al6061-T4

Material	Young's modulus (GPa)	Poisson's ratio	Yield stress (MPa)	Hardening law (MPa)	Critical damage (normalized C&L)
Al6061-T4	68.9	0.28	168.1	$\overline{\sigma} = 538\overline{\varepsilon}^{0.172}$	C = 1.61

$$[x_1, x_2 \cdots x_{16}] = [0.6, 88, 0.3, 3.8, 0.5, 1.9, 0.2, 0.08, 0.6, 0.4, 0.4, 0.7, 1.9, 0.7, 1.1, 0.45] \quad (14)$$

All individuals and best individuals in each generation are shown in Fig. 10 to investigate the evolutionary process. As is shown in Fig. 10, all individuals are gradually get together. With the increase of the generation, the best individual is gradually close to optimum curve ($F_{fr} = F_{se}$) and the location of the best individual is gradually close to the upper right corner where F_{fr} and F_{se} are simultaneously big. In addition, all individuals are gradually converging toward the best individual with the increase of generation. It is indicated that the algorithm is gradually converged with the increase of generation. This fact is strongly agreed with the inference once again.

The best shape of the clinching tools at each generation is illustrated in Fig. 11 to understand the evolutionary process easily. The maximum damage of the sheets is far less than critical value of 1.61 at each generation, which ensures that the joint will not crack in the clinching process. The outline of the die groove has two troughs at 1st generation (see Fig. 11a). With the increase of the evolutionary generation, the outline of the die groove is more and more smooth, and finally close to an arc. In addition, the outline of the die groove is not contacted with the lower sheet at the beginning, and then the clearance between the lower sheet and the outline of the die groove is gradually close to zero. These phenomena will be validated in the next section.

The evolutionary tendency of the design variables is shown in Fig. 12. Although the change of the design variables is little, especially for x_{13}, the change of the axial strength is very large. The fact indicates that the sensitiveness of each variable is not equal. In addition, the change of a single variable does not show a certain regularity. In other words, the changes of the design variables are mutually coordinated in the optimization process. These design variables must be taken into account simultaneously in the optimization process. Therefore, it is difficult to use surrogate model (ANN, RSM, etc.) to approximate the response relationship between design variables and design objective (Fig. 13).

4.2 Shape validation

As in the above analysis, there are two questions: whether the outline of die groove is arc, and whether the clearance between lower sheet and the outline of die groove is equal to zero to obtain the best joint. In order to answer these questions, four new optimization processes which have different initial tools' shape were performed. The design variables were assigned as x_7, x_8, x_9, x_{10}, and x_{11}, and the other variables were set as the optimized value, by which the effects of other parameters can be entirely eliminated. Four typical initial shapes of die groove are shown in Fig. 15a–p. Particularly, the initial shape 4 is automatically assigned by the computer. The population size can be reduced from 100 to 20 because of the reduction of the design variables. After 20 generations' evolution (400 times of simulation) for each initial shape, the optimization process can be terminated, because the fitness is unimproved after 15th generation (see Fig. 13).

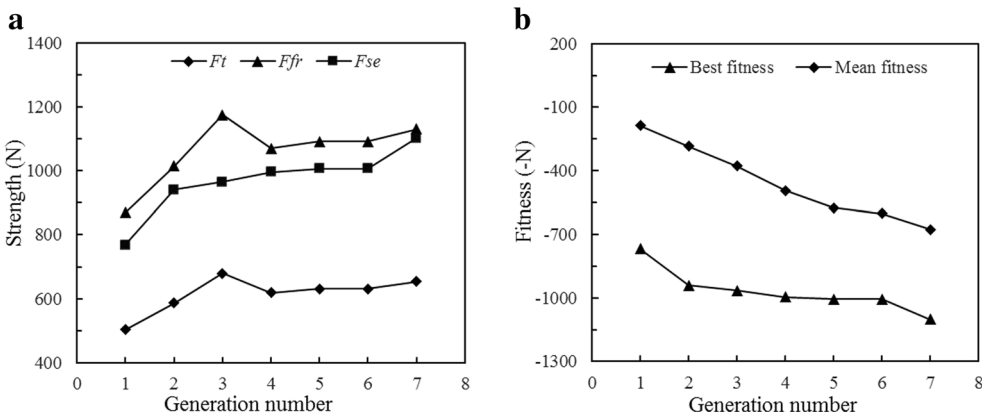

Fig. 9 Evolutionary tendency of joint strength (**a**) and fitness (**b**)

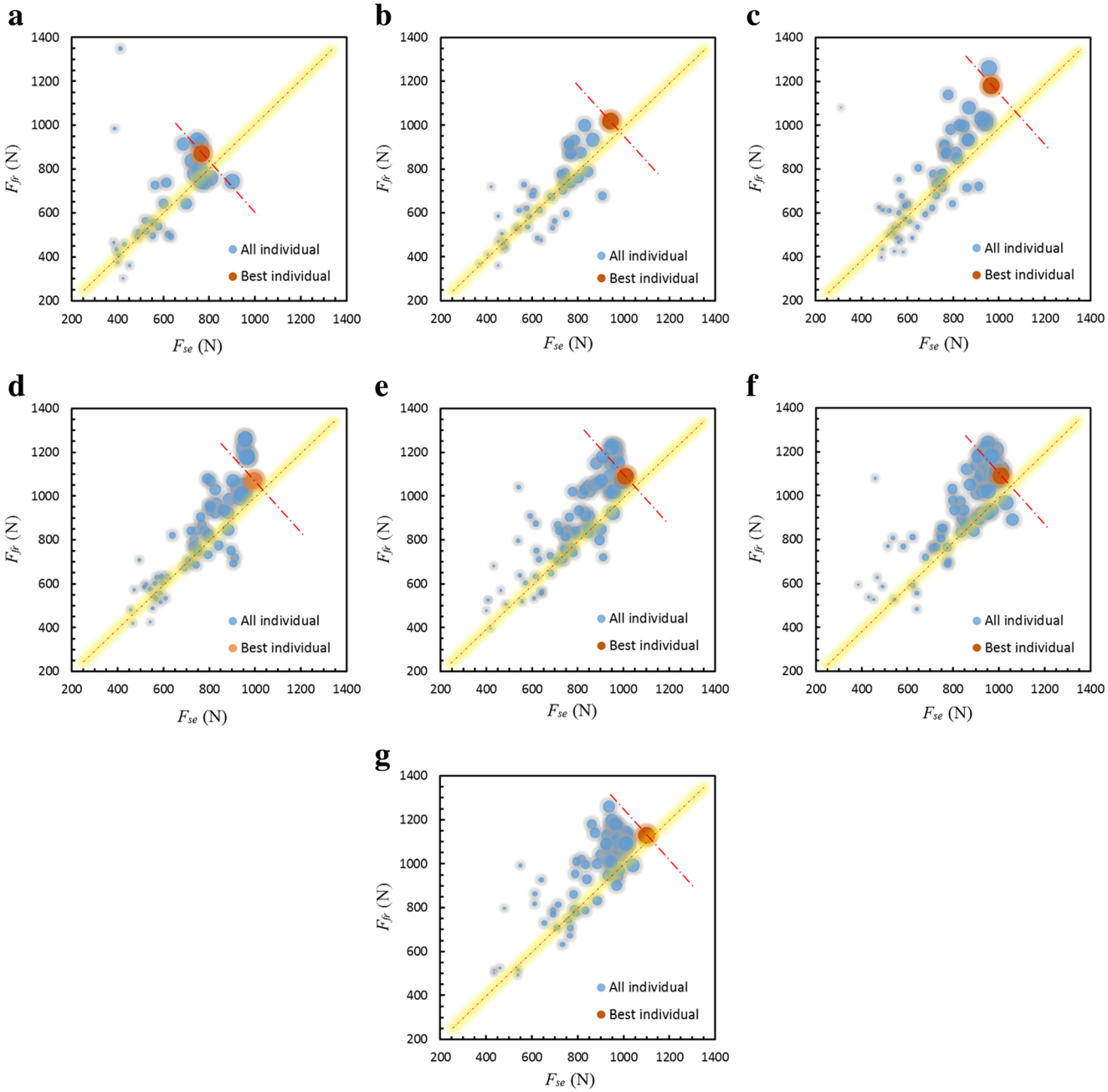

Fig. 10 Individual distribution at 1st generation (**a**), 2nd generation (**b**), 3rd generation (**c**), 4th generation (**d**), 5th generation (**e**), 6th generation (**f**), and 7th generation (**g**)

The optimized strength for four types is very similar regardless of the initial die shape. In other words, the initial shape of the die groove has a little effect on the solution results. Different initial shapes need different computing generation to obtain optimum results, especially, initial shape 4 (randomly assigned by computer) needs more evolutionary generation. Therefore, a better initial shape can significantly reduce the evolutionary generation. In order to investigate the evolutionary process for all individuals, the individual distribution of four initial shapes for all generations is shown in Fig. 14.

Although the individual distribution for four initial shapes is different, the location of the final optimized result is very close to each other (see Fig. 14). This fact proves, to some extent, that the final optimized results are the global optimal solution. In addition, this also suggests that initial shape of the die groove determines the starting point and the evolutionary direction but not the final results. As shown in Fig. 14a, c, a good initial shape is easy to get the global optimum point, which indicates that a good initial shape can save the optimization time and also can increase the possibility of finding the best individual. Hence, the initial shape of clinching tools

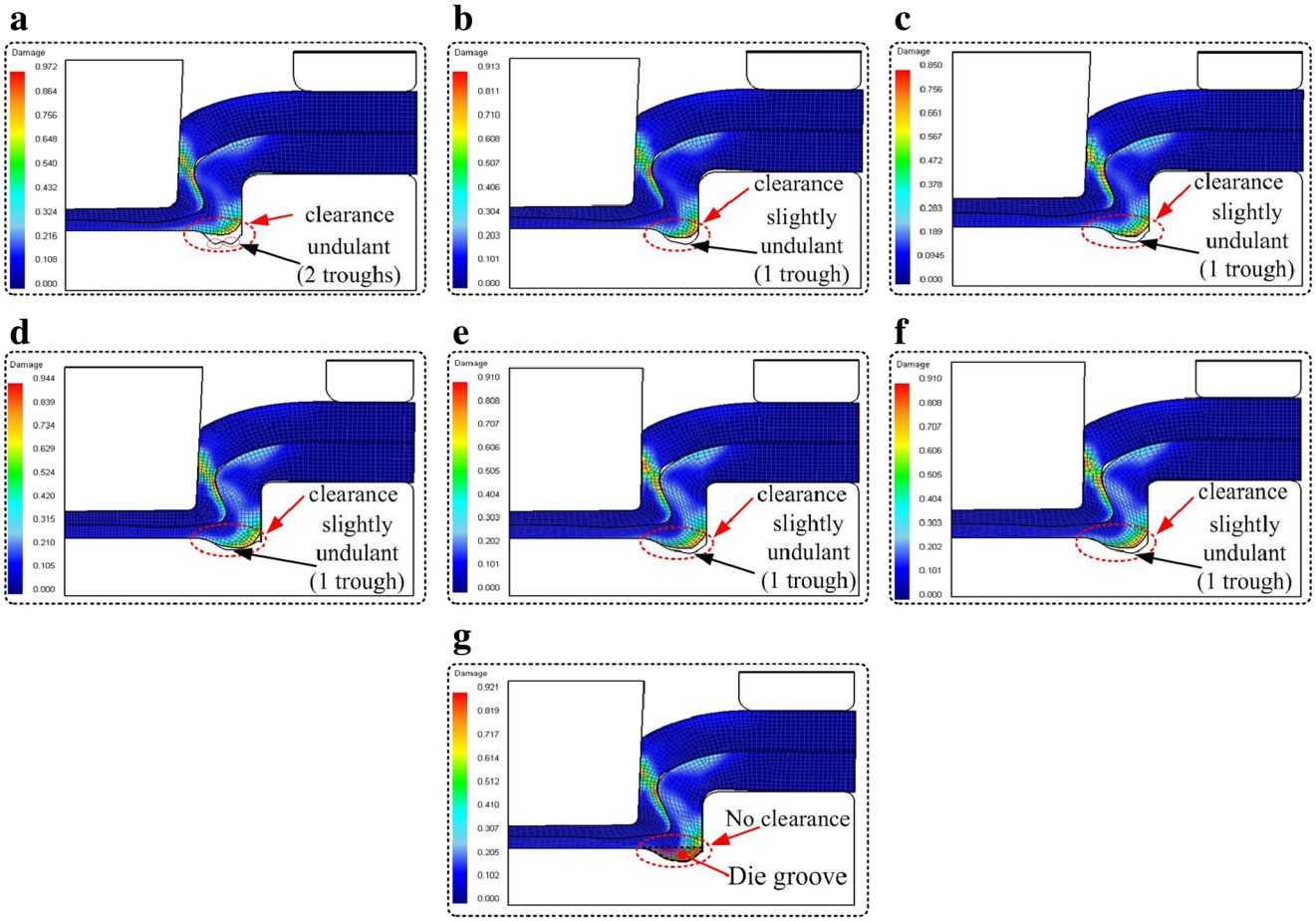

Fig. 11 The shape of the best individual at 1st generation (**a**), 2nd generation (**b**), 3rd generation (**c**), 4th generation (**d**), 5th generation (**e**), 6th generation (**f**), and 7th generation (**g**)

should be specified as much as possible in practical applications.

The shape evolution of the die groove is shown in Fig. 15 to investigate the most suitable shape. The evolutionary

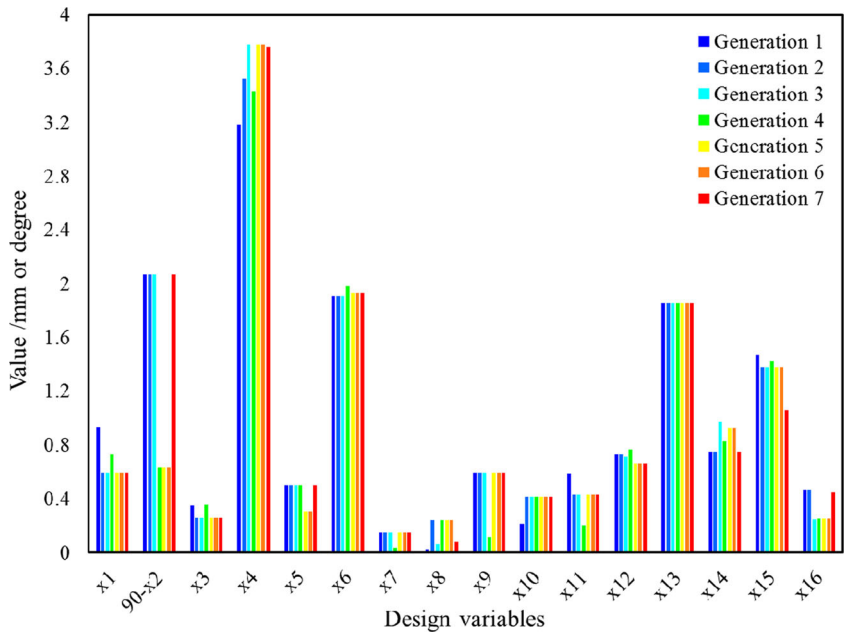

Fig. 12 Evolutionary tendency for design variables

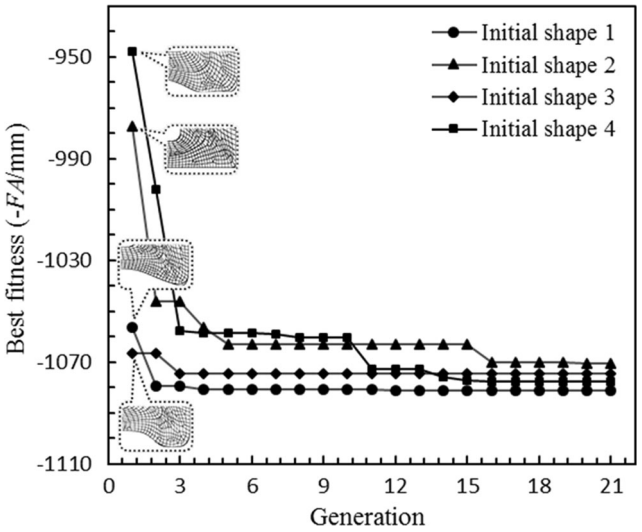

Fig. 13 Fitness curves for four initial shapes

results indicate that the final shapes of die groove for four initial shapes are a smooth curve which is similar to arc curve (see Fig. 15e–s). In other words, the effect of the initial shape of die groove on the final shape of die groove is not significant. As shown in Fig. 15f, there is no groove in the initial shape, but the final shape has a groove. Therefore, the die groove is necessary to obtain the strongest joint (see Fig. 15f–j), and the die groove should be smooth enough.

In addition to the shape of die groove, the clearance between upper sheet and die groove is also very important. As is shown in Fig. 15, the clearances for four initial shapes are gradually close to zero after 20th generation (see Fig. 15e–s). These results suggest that the clearance should be equal to zero to obtain strongest joint. However, it is not necessary to elaborate the die groove for general applications, because the improvement of the joint strength is less than 50 N from 3rd generation to 20th generation. The results indicate that the shape of the die groove can be replaced by arc curve to simplify the structure of the clinching tools for general applications. If the requirement of the joint strength is very high, the clearance between the lower sheet and the die groove should be equal to zero. But for ordinary applications, the zero clearance is not necessary.

4.3 Mechanism analysis

The preceding results show that the outline of the die groove should be smooth enough and the clearance between the lower sheet and the outline of the die groove should be close to zero. The flow behavior of materials is shown in Fig. 16. The flow

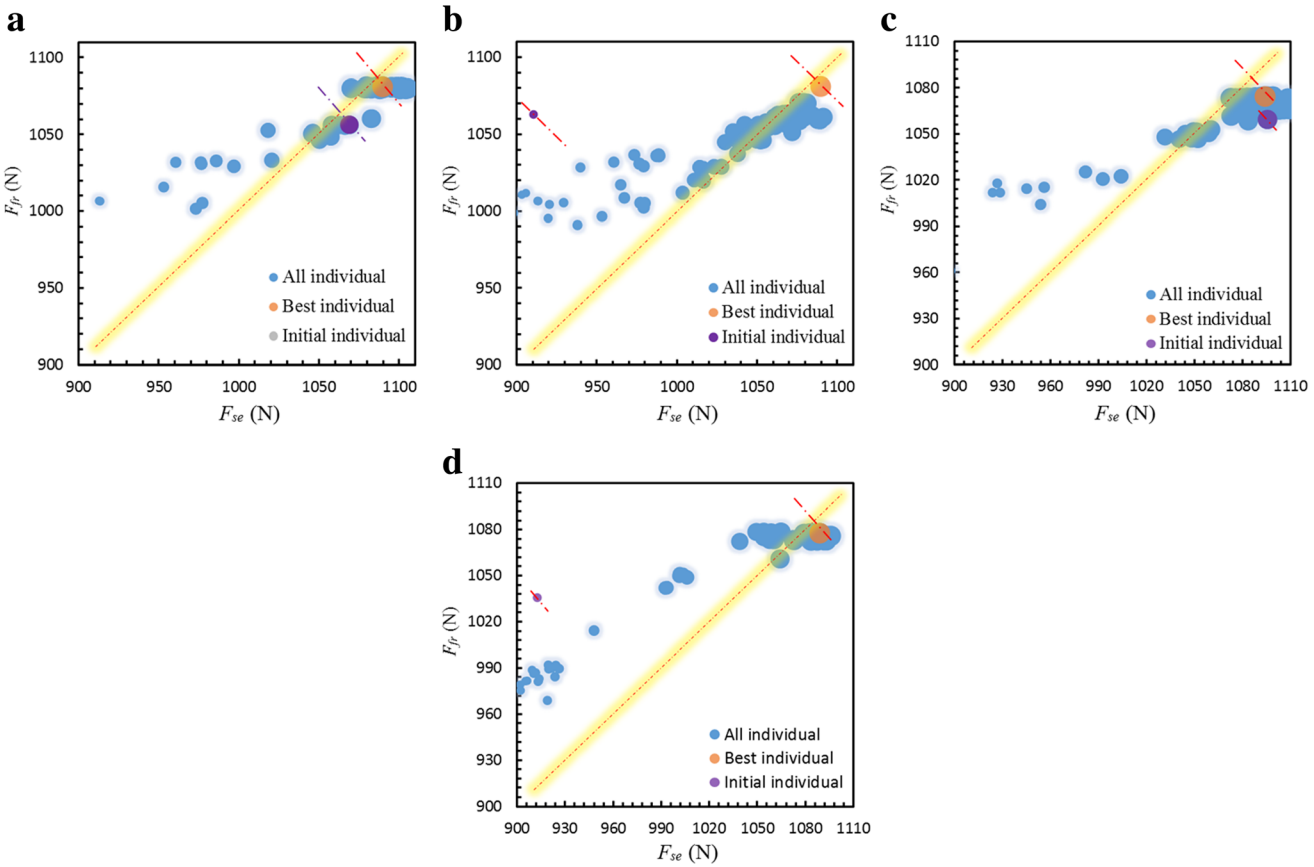

Fig. 14 Individual distribution for initial shapes 1 (**a**), initial shapes 2 (**b**), initial shapes 3 (**c**), initial shapes 4 (**d**)

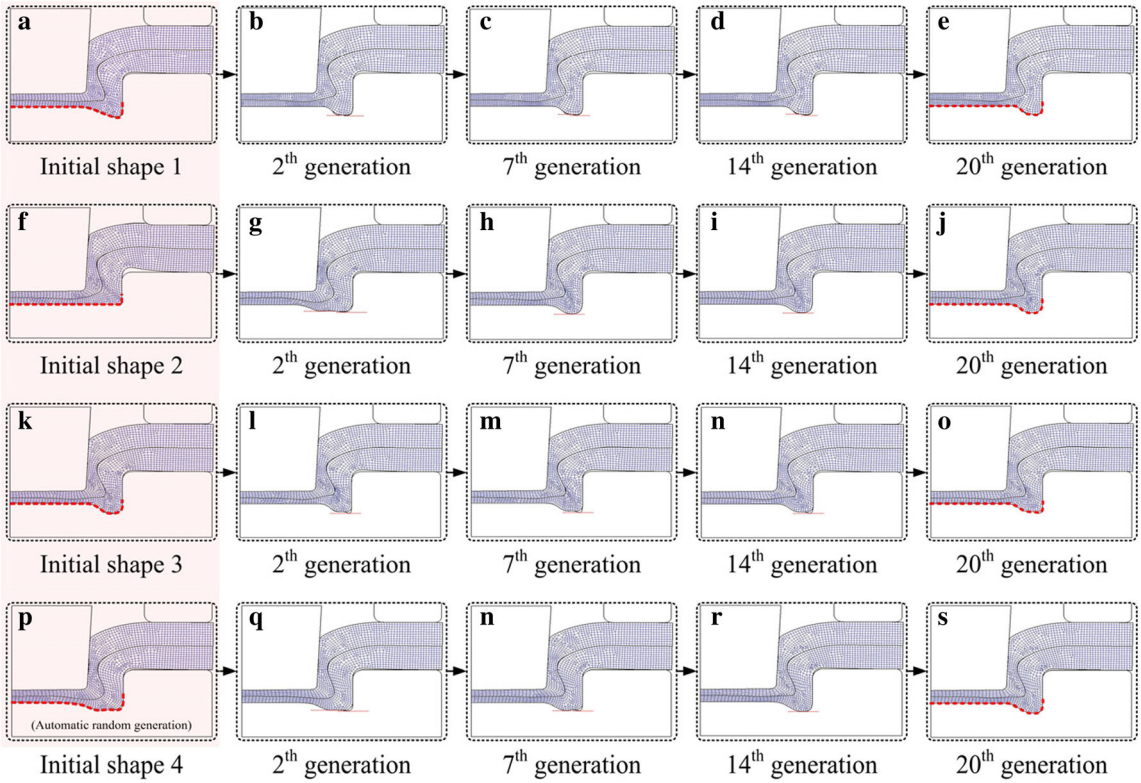

Fig. 15 Best individual at key generation for different initial shapes

of material can be divided into two directions: axial direction and radial direction. It is difficult that the metal in III′ flows to the left (because of the pressure from VI). Therefore, the formation of the interlocking region must depend on the metal in II′ which flows to the right. The flow of the metal in VI′ region along axial direction is very limited because of the constraint of the holder. Therefore, a space is needed to accommodate the extra materials from the interlocking region, which is why the die groove has been formed in the optimization process. The metal in the V′ region must be flowed into the die groove. The smooth curve is conducive to the flow of the material, because the resistance formed by the smooth shape is far less than the multi-peak curve. This is why the arc outline of the die groove is formed in the optimization process. According to the above analysis, the die groove is necessary to form interlocking region and the outline of the die groove should be smooth enough.

In addition, there is a phenomenon that the clearance between the lower sheet and the outline of the die groove is gradually close to zero in the optimization process. The zero gap between the lower sheet and the die groove can lead to a contact anti-pressure. The anti-pressure can improve the formability of the materials, because the state of compressive stress can improve the plasticity of materials. The high-integrity clinched joint is easier to obtain because of the existence of this contact counter pressure. This is why the gap between the lower sheet and the outline of the die groove is gradually close to zero in the optimization process.

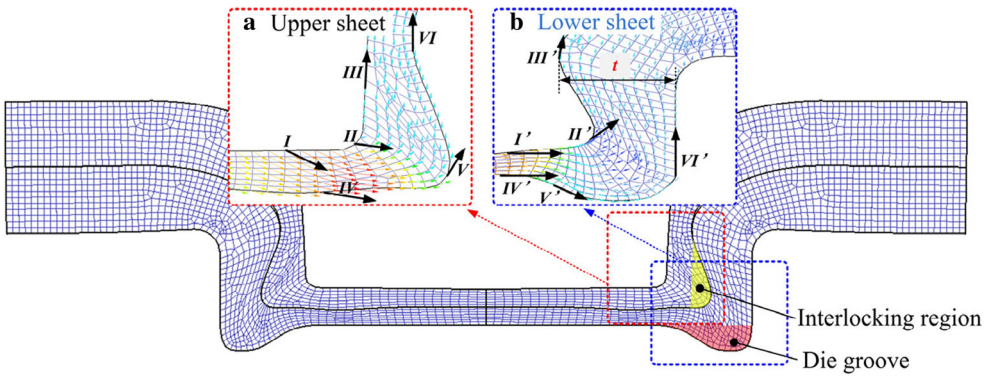

Fig. 16 Flow behavior of material for upper and lower sheets (best joint at the 20th generation)

5 Conclusions

In this paper, a methodology for optimizing clinched joint has been established. An optimization system, which can automatically complete the optimization process, has been developed based on this methodology. In addition, the rule of the shape evolutionary is investigated to simplify the structure, and Al6061-T4 sheets are used to test the optimization methodology. According to the optimized and analyzed results, the main conclusions have been listed as follows:

(1) The optimization methodology is a convenient way to optimize the strength of the clinched joint. The direct communication between FEM and GA is an efficient way to solve this multi-variable global optimization problem. This optimization methodology can be directly applied to the optimization of this kind of joint.
(2) The axial strength of the clinched joint can be increased from 767 to 1100 N, and the shear strength of clinched joint is increased from 500 to 652 N by using this methodology. Although the shear strength, which was translated into constraint conditions, is less than the axial strength, the total shear strength can be increased by using more clinch joints in practical application. In fact, the strength optimization of clinched joint is to deal with the balance between two kinds of axial strength.
(3) According to the shape evolution of the Bezier curve for four initial shapes, the die groove must be given and the shape of the die groove should be smooth enough to obtain the strongest joint, particularly the arc curve can be used to simplify structure of the die groove. In addition, the clearance between upper sheet and die groove should be equal to zero if the required joint strength is very high, and it is not necessary if the required joint strength is not very high.

References

1. Lee CJ, Kim JY, Lee SK, Ko DC, Kim BM (2010) Parametric study on mechanical clinching process for joining aluminum alloy and high-strength steel sheets. J Mech Sci Technol 24(1):123–126
2. He X, Pearson I, Young K (2008) Self-pierce riveting for sheet materials: state of the art. J Mater Process Technol 199(1–3):27–36
3. Lambiase F (2013) Influence of process parameters in mechanical clinching with extensible dies. Int J Adv Manuf Technol 66(9): 2123–2131
4. He X (2010) Recent development in finite element analysis of clinched joints. Int J Adv Manuf Technol 48(5):607–612
5. Lee C-J, Kim J-Y, Lee S-K, Ko D-C, Kim B-M (2010) Design of mechanical clinching tools for joining of aluminium alloy sheets. Mater Des 31(4):1854–1861
6. Abe Y, Kato T, Mori KI, Nishino S (2014) Mechanical clinching of ultra-high strength steel sheets and strength of joints. J Mater Process Technol 214(10):2112–2118
7. He X, Zhang Y, Xing B, Gu F, Ball A (2015) Mechanical properties of extensible die clinched joints in titanium sheet materials. Mater Des 71:26–35
8. Neugebauer R, Kraus C, Dietrich S (2008) Advances in mechanical joining of magnesium. CIRP Ann Manuf Technol 57(1):283–286
9. Lambiase F (2015) Mechanical behaviour of polymer–metal hybrid joints produced by clinching using different tools. Mater Des 87: 606–618
10. Lambiase F (2015) Joinability of different thermoplastic polymers with aluminium AA6082 sheets by mechanical clinching. Int J Adv Manuf Technol 80(9):1995–2006
11. Lambiase F, Ilio AD (2015) Mechanical clinching of metal–polymer joints. J Mater Process Technol 215:12–19
12. Lambiase F, Durante M, Ilio AD (2016) Fast joining of aluminum sheets with glass fiber reinforced polymer (GFRP) by mechanical clinching. J Mater Process Technol 236:241–251
13. Lambiase F, Ko DC (2016) Feasibility of mechanical clinching for joining aluminum AA6082-T6 and carbon fiber reinforced polymer sheets. Mater Des 107:341–352
14. Lee SH, Lee CJ, Lee KH, Lee JM, Kim BM, Ko DC (2014) Influence of tool shape on hole clinching for carbon fiber-reinforced plastic and SPRC440. Adv Mech Eng 2014(2): 810864–810864
15. Lambiase F (2015) Clinch joining of heat-treatable aluminum AA6082-T6 alloy under warm conditions. J Mater Process Technol 225:421–432
16. Osten J, Söllig P, Reich M, Kalich J, Füssel U, Kessler O (2014) Softening of high-strength steel for laser assisted clinching. Adv Mater Res 966-967:617–627
17. Abe Y, Nihsino S, K-i M, Saito T (2014) Improvement of joinability in mechanical clinching of ultra-high strength steel sheets using counter pressure with ring rubber. Procedia Eng 81:2056–2061
18. Mucha J (2011) The analysis of lock forming mechanism in the clinching joint. Mater Des 32(10):4943–4954
19. Varis JP (2003) The suitability of clinching as a joining method for high-strength structural steel. J Mater Process Technol 132(1–3): 242–249
20. Lambiase F, Di Ilio A (2016) Damage analysis in mechanical clinching: experimental and numerical study. J Mater Process Technol 230:109–120
21. Oudjene M, Ben-Ayed L (2008) On the parametrical study of clinch joining of metallic sheets using the Taguchi method. Eng Struct 30(6):1782–1788
22. Lambiase F, Di Ilio A (2013) Optimization of the clinching tools by means of integrated FE modeling and artificial intelligence techniques. Procedia CIRP 12:163–168
23. Roux E, Bouchard PO (2013) Kriging metamodel global optimization of clinching joining processes accounting for ductile damage. J Mater Process Technol 213(7):1038–1047
24. Oudjene M, Ben-Ayed L, Delamézière A, Batoz JL (2009) Shape optimization of clinching tools using the response surface methodology with moving least-square approximation. J Mater Process Technol 209(1):289–296
25. Lebaal N, Oudjene M, Roth S (2012) The optimal design of sheet metal forming processes: application to the clinching of thin sheets. Int J Comput Appl Technol 43(2):110–116
26. Coppieters S, Lava P, Baes S, Sol H, Van Houtte P, Debruyne D (2012) Analytical method to predict the pull-out strength of clinched connections. Thin-Walled Struct 52:42–52
27. Varis JP, Lepistö J (2003) A simple testing-based procedure and simulation of the clinching process using finite element analysis for establishing clinching parameters. Thin-Walled Struct 41(8): 691–709

28. Lee C-J, Lee J-M, Ryu H-Y, Lee K-H, Kim B-M, Ko D-C (2014) Design of hole-clinching process for joining of dissimilar materials—Al6061-T4 alloy with DP780 steel, hot-pressed 22MnB5 steel, and carbon fiber reinforced plastic. J Mater Process Technol 214(10):2169–2178
29. Hambli R, Reszka M (2002) Fracture criteria identification using an inverse technique method and blanking experiment. Int J Mech Sci 44(7):1349–1361
30. Lee CJ, Kim JY, Lee SK (2010) Parametric study on mechanical clinching process for joining aluminum alloy and high-strength steel sheets. J Mech Sci Technol 24(1):123–126
31. Rouffaud R, Hladky-Hennion AC, Levassort F (2017) A combined genetic algorithm and finite element method for the determination of a practical elasto-electric set for 1-3 piezocomposite phases. Ultrasonics 77:214–223